



# Modelling of the optimum cooling condition in two-dimensional solidification processes

**D. Słota\***

Institute of Mathematics, Silesian University of Technology,  
ul. Kaszubska 23, Gliwice 44-100, Poland

\* Corresponding author: E-mail address: damian.slota@polsl.pl

Received in a revised form 15.12.2007; published 02.01.2009

## ABSTRACT

**Purpose:** This paper presents the method of the calculation of the cooling condition in the two-dimensional solidification processes.

**Design/methodology/approach:** The considered problem consists in the reconstruction of the function that describes the heat transfer coefficient on the boundary, when the temperature measurements in selected points of the solid phase are well-known. In calculations the alternating phase truncation method, the genetic algorithm and the Tikhonov regularization were used.

**Findings:** The calculations show a very good approximation of the exact solution and the stability of the procedure.

**Research limitations/implications:** On the bases of the results that every start-up of the genetic algorithm leads to similar results, which are reflected by very low values of the standard deviation.

**Originality/value:** The calculations point to the stability of the proposed method in view of the input data errors, number of control points, substantiating the usability of such approach.

**Keywords:** Solidification; Inverse Stefan problems; Genetic algorithm; Tikhonov regularization

**Reference to this paper should be given in the following way:**

D. Słota, Modelling of the optimum cooling condition in two-dimensional solidification processes, Archives of Computational Materials Science and Surface Engineering 1/1 (2009) 45-52.

## METHODS OF ANALYSIS AND MODELLING

### 1. Introduction

Two-phase Stefan problem is a model of the solidification of pure metals. In this problem the distribution of temperature in solid and liquid phase are described by the heat conduction equation with initial and boundary conditions. Whereas the position of the freezing front is described by the Stefan conditions and the condition of temperature continuity. The inverse Stefan problem consist in the determination of the initial conditions, boundary conditions or thermophysical properties of a body. However, the insufficiency of input information is compensated by some additional information on the effects of the input

conditions. For the inverse Stefan problem this additional information is the position of the freezing front, its velocity in normal direction or temperature in selected points of the domain. The problems in which the additional information is the position of the freezing front are called design problems.

A majority of available studies refer to the one-dimensional inverse Stefan problem [4,6,10], whereas studies regarding the two-dimensional inverse Stefan problem are scarce. In the first study concerning the two-dimensional inverse design Stefan problem Colton [1] determined the temperature at the boundary of the domain, in the form of a series of integrals, based on the known interface position. Jochum [7] treats the two-dimensional

one-phase inverse Stefan problem as a problem of the non-linear approximation theory. The task consists in a selection of a particular heat flux, which will minimize the functional defined as the norm of difference between the given interface position and the position reconstructed for the given heat flux. The two-dimensional problem is also discussed by Zabarás *et al.* [18, 19] and Kang and Zabarás [8]. In these papers the heat flux or the temperature is determined on the boundary of the domain when the interface velocity is known.

Two-dimensional two-phase inverse design Stefan problem is considered also by Grzymkowski and Słota [2,3,4]. Grzymkowski and Słota [3] found the solution in a linear combination form of the functions satisfying the equation of heat conduction. The coefficients of this combination are determined by the least square method to minimize the maximal defect in the initial-boundary data. The next method described by Grzymkowski and Słota [2,4] consists of the minimization of a functional, the value of which is the norm of a difference between given positions of the moving interfaces of the phase change and positions reconstructed from the selected function describing the heat transfer coefficient.

This paper presents the method of the calculation of the cooling condition in the two-dimensional inverse Stefan problem. The considered problem consists of the reconstruction of the function describing the heat transfer coefficient on the boundary, when the temperature measurements in selected points of the solid phase are well-known. In numerical calculations the alternating phase truncation method [11,14] the Tikhonov regularization [9,17] and the genetic algorithm [12,13] were used. The featured examples of calculations show a very good approximation of the exact solution and the stability of the procedure. The application of a genetic algorithm to one-dimensional inverse design Stefan problem is considered in other papers [15,20].

## 2. Two-dimensional problem

Let  $\Omega = [0, b] \times [0, d]$  and on the boundary of domain  $D = \Omega \times [0, t^*]$ , five components are distributed (Fig. 1):

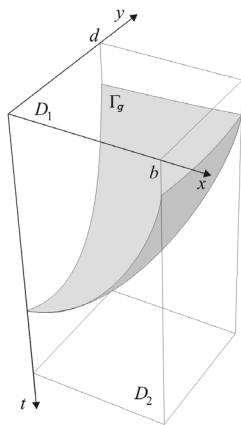


Fig. 1. Domain of the two-dimensional problem

$$\begin{aligned}\Gamma_0 &= \{(x, y, 0), x \in [0, b], y \in [0, d]\}, \\ \Gamma_1 &= \{(0, y, t), y \in [0, d], t \in [0, t^*]\}, \\ \Gamma_2 &= \{(x, 0, t), x \in [0, b], t \in [0, t^*]\}, \\ \Gamma_3 &= \{(b, y, t), y \in [0, d], t \in [0, t^*]\}, \\ \Gamma_4 &= \{(x, d, t), x \in [0, b], t \in [0, t^*]\},\end{aligned}$$

where initial condition and boundary conditions are given. Let  $D_1$  denote the subset of domain  $D$ , which is occupied by a liquid phase, and let  $D_2$  denote the domain occupied by a solid phase.

The liquid and solid phase are separated by the freezing front  $\Gamma_g$ .

We will look for an approximate solution of the problem with the known values of temperatures in selected points of the solid phase ( $(x_i, y_i, t_j) \in D_2$ ):

$$T_2(x_i, y_i, t_j) = U_{ij}, \quad i = 1, 2, \dots, N_1, \quad j = 1, 2, \dots, N_2, \quad (1)$$

where  $N_1$  means the number of sensors and  $N_2$  means the number of measurements from each sensor. Function  $\alpha(t)$  defined on boundaries  $\Gamma_3$  and  $\Gamma_4$  is to be determined, and position of the freezing front  $\Gamma_g$  and the distribution of temperatures  $T_k$  in domains  $D_k$  ( $k = 1, 2$ ), which inside domains  $D_k$  ( $k = 1, 2$ ) fulfil the heat conduction equation:

$$c_k \rho_k \frac{\partial T_k}{\partial t}(x, y, t) = \lambda_k \nabla^2 T_k(x, y, t), \quad (2)$$

on boundary  $\Gamma_0$ , they fulfil the initial condition ( $T_0 > T^*$ ):

$$T_1(x, y, 0) = T_0, \quad (3)$$

on boundaries  $\Gamma_1$  and  $\Gamma_2$ , they fulfil the homogeneous second kind boundary conditions:

$$-\lambda_k \frac{\partial T_k}{\partial n}(x, y, t) = 0, \quad (4)$$

on boundaries  $\Gamma_3$  and  $\Gamma_4$ , they fulfil the third kind boundary conditions:

$$-\lambda_k \frac{\partial T_k}{\partial n}(x, y, t) = \alpha(x, y, t)(T_k(x, y, t) - T_\infty), \quad (5)$$

whereas on the freezing front  $\Gamma_g$ , they fulfil the temperature continuity condition and the Stefan condition:

$$T_1(x, y, t)|_{\Gamma_g} = T_2(x, y, t)|_{\Gamma_g} = T^*, \quad (6)$$

$$-\lambda_1 \frac{\partial T_1(x, y, t)}{\partial n} \Big|_{\Gamma_g} + \lambda_2 \frac{\partial T_2(x, y, t)}{\partial n} \Big|_{\Gamma_g} = L \rho_2 \mathbf{v}_n, \quad (7)$$

where  $c_k$ ,  $\rho_k$  and  $\lambda_k$  are the specific heat, the mass density and the thermal conductivity in the liquid phase ( $k = 1$ ) and solid phase ( $k = 2$ ), respectively,  $\alpha$  is the heat transfer coefficient,  $T_0$  is the initial temperature,  $T_\infty$  is the ambient temperature,  $T^*$  is the temperature of solidification,  $L$  is the latent heat of fusion,  $\mathbf{v}_n$  is the freezing front velocity vector in a normal direction, and  $t$ ,  $x$  and  $y$  refer to time and spatial locations, respectively.

Function  $\alpha(x, y, t)$ , describing the heat transfer coefficient, will be sought in the form of a function dependent (in a linear or non-linear way) on  $n$  parameters:

$$\alpha(x, y, t) = \alpha(x, y, t; \alpha_1, \alpha_2, \dots, \alpha_n). \quad (8)$$

Let  $V_\alpha$  denotes a set of all functions in the form of (8), where  $\alpha_i \in [\alpha_i^l, \alpha_i^u]$  for  $i = 1, 2, \dots, n$ .

For the determined function  $\alpha(x, y, t) \in V_\alpha$ , the problem (2)-(7) becomes a direct Stefan problem, the solution of which allows finding the courses of temperatures  $T_{ij} = T_2(x_i, y_i, t_j)$  corresponding to function  $\alpha(x, y, t)$ . By taking advantage of the calculated temperatures  $T_{ij}$  and the given temperatures  $U_{ij}$ , we can build a functional which will determine the error of the approximate solution:

$$J(\alpha(t)) = \|T - U\|^2 + \gamma \|\alpha\|^2, \quad (9)$$

where  $\gamma$  is the regularization parameter and

$$\|T - U\|^2 = \sum_{i=1}^{N_1} \sum_{j=1}^{N_2} (T_{ij} - U_{ij})^2, \quad (10)$$

$$\|\alpha\|^2 = \int_S \omega(r) (\alpha(r))^2 dt, \quad (11)$$

$\omega(t)$  is a weight function,  $S = \Gamma_3 \cup \Gamma_4$ , and  $r$  is a point of surface  $S$ . To determine the regularization parameter, the discrepancy principle proposed by Morozov was used [9, 17].

### 3. Genetic algorithm

To find the Tikhonov functional minimum, a genetic algorithm was used. For the representation of the vector of decision variables, a chromosome was used in the form of a vector of real numbers [12, 13]. The tournament selection and elitist model were applied in the algorithm. This selection is carried out so that two chromosomes are drawn and the one with better fitness, goes to a new generation. There are as many draws as individuals that the new generation is supposed to include. In the elitist model the best individual of the previous generation is saved and, if all individuals in the current generation are worse, the worst of them is replaced with the saved best individual from the previous population. As the crossover operator, arithmetical crossover was applied, where as a result of crossing of two chromosomes, their linear combinations are obtained. In the calculations, a nonuniform mutation operator was used as well. In calculations parameters used for the genetic algorithm are as follows: population size  $n_{pop} = 70$ , number of generations  $N = 1000$ , crossover probability  $p_c = 0.7$ , mutation probability  $p_m = 0.1$ .

### 4. Calculation example

Now we will present an example illustrating the accuracy and stability of the presented algorithm. In the presented example, the following values were assumed for the parameters:

$b = d = 0.08$  [m],  $\lambda_1 = 33$  [W/(m K)],  $\lambda_2 = 30$  [W/(m K)],  $c_1 = 800$  [J/(kg K)],  $c_2 = 690$  [J/(kg K)],  $\rho_1 = 7000$  [kg/m<sup>3</sup>],  $\rho_2 = 7500$  [kg/m<sup>3</sup>],  $L = 270000$  [J/kg],  $T^* = 1773$  [K],  $T_\infty = 323$  [K] and  $T_0 = 1813$  [K].

Function  $\alpha(x, y, t) = \alpha(x, y, t; \alpha_1, \alpha_2, \alpha_3, \alpha_4, \alpha_5, \alpha_6)$  was sought in the form:

$$\alpha(x, y, t) = \begin{cases} \alpha_1 & \text{for } t \in [0, t_1], \quad x \in [0, b], \quad y = d, \\ \alpha_3 & \text{for } t \in (t_1, t_2], \quad x \in [0, b], \quad y = d, \\ \alpha_5 & \text{for } t > t_2, \quad x \in [0, b], \quad y = d, \\ \alpha_2 & \text{for } t \in [0, t_1], \quad x = b, \quad y \in [0, d], \\ \alpha_4 & \text{for } t \in (t_1, t_2], \quad x = b, \quad y \in [0, d], \\ \alpha_6 & \text{for } t > t_2, \quad x = b, \quad y \in [0, d], \end{cases}$$

where  $t_1 = 38$  [s],  $t_2 = 93$  [s]. The exact values of the coefficients  $\alpha_i$  amounts to:

$$\alpha_1 = 1200, \quad \alpha_3 = 800, \quad \alpha_5 = 250,$$

$$\alpha_2 = 800, \quad \alpha_4 = 500, \quad \alpha_6 = 250.$$

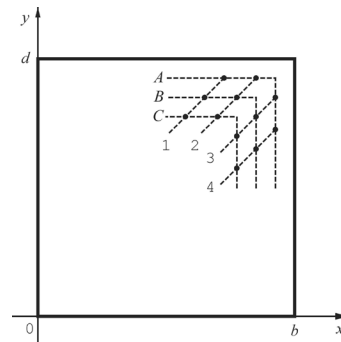


Fig. 2. Positions of the measurement points

Direct Stefan problem was solved by applying the alternating phase truncation method. In the alternating phase truncation method, the finite-difference method was used, with the calculations made on a grid of discretization intervals equal  $\Delta t = 0.1$ ,  $\Delta x = b/100$  and  $\Delta y = d/100$ . A (reasonable) change of the grid density did not have any significant influence on the results obtained.

It was also assumed that the temperature values are known at four points ( $N_1 = 4$ ), i.e. in the considered domain there are four thermocouples placed at the distance of 4 [mm] (A), 8 [mm] (B) or 12 [mm] (C) from the domain boundary (Fig. 2). Temperature readings were taken every 1 [s], 2 [s], 4 [s] and 8 [s], which corresponded to the circumstances under which 200, 100, 50 or 25 temperature measurements were made for every thermocouple. The calculations were made for accurate values of the temperature measurements and for values disturbed with a pseudorandom error of normal distribution. Results for 1% and 2% disturbance are presented in the paper. In each case, calculations were carried out for five different initial settings of a pseudorandom numbers generator.

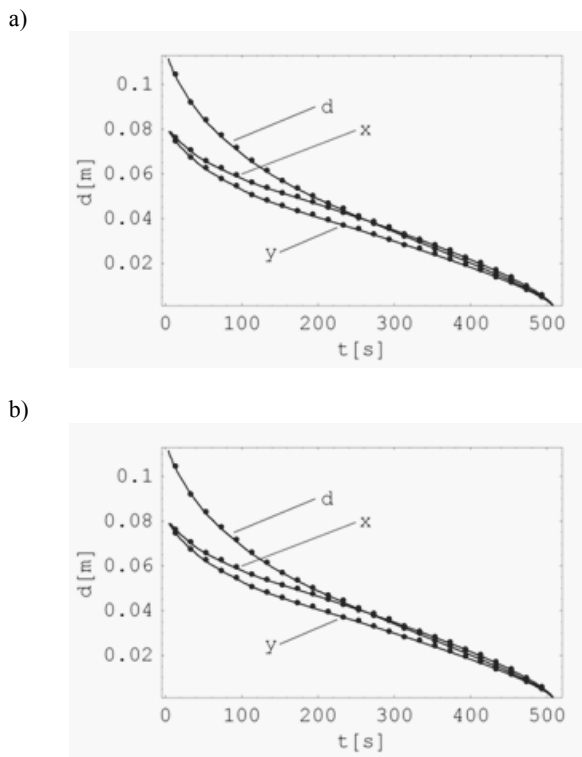


Fig. 3. Exact (solid line) and reconstructed (dots) position of the freezing front for the calculation for the sensors in position C, perturbation equal to 2%, and for the temperature control performed every two seconds (a) and every eight seconds (b) (x - section of the freezing front with plane  $y=0$ , y - section of surface of the freezing front with plane  $x=0$ , p - section of the freezing front with plane  $y=x$ )

In Fig. 3 the exact and reconstructed position of the freezing front were plotted for the sensors in position C, perturbation equal to 2% and temperature readings every two and eight seconds. The freezing front  $\Gamma_g$  is located alongside three cross-sections: with plane  $y=0$ , plane  $x=0$  and plane  $y=x$ . In other cases, the location of the freezing front was reconstructed with very good exactness.

The results of the reconstruction of the heat transfer coefficient at various zones for the sensors in position C are compiled in Tables 1 and 2. The Tables also state the errors with which the coefficients were reconstructed, and the last two columns contain the standard deviation and its values expressed as the weighted average percentage. The errors in reconstructing the heat transfer coefficient for the sensors in position A and B are shown in Figs. 4 and 5. In the case of detailed input data, the heat transfer coefficient is reconstructed with minimal errors (not exceeding 0.06%), which may be further reduced by changing the criterion of ending the genetic algorithm (increasing the maximal number of generations). The highest values of the errors were derived for the sensors in position C, i.e. as far from the domain boundary as possible. For disturbed input data, however, the errors never exceed the values of reconstructing the heat transfer coefficient at the input, or, in most cases, were even lower. Apart from the position, the values of the errors are also affected by the number of control points (the points at which the temperature values are known) and the errors in the input data. The reduction of the number of the control points and increase of the size of the errors generally result in worse reconstruction of the heat transfer coefficient. The results indicate that the successive start-ups of the genetic algorithm end in similar results, which is reflected in very low values of the standard deviation.

Table 1. Results of the calculations for the sensors in position C ( $\alpha$  - reconstructed values of the heat transfer coefficient,  $e$  - relative percentage error,  $\sigma$  - standard deviation,  $\sigma^p$  - standard deviations in percent of mean value)

Per.	$\alpha$	$e$ [%]	$\sigma$	$\sigma^p$ [%]	$\alpha$	$e$ [%]	$\sigma$	$\sigma^p$ [%]
	1s				2s			
0%	1200.09	0.007133	0.690049	0.057500	1199.88	0.009867	0.561180	0.046770
	800.03	0.003675	0.700577	0.087569	800.13	0.015625	0.548626	0.068568
	250.03	0.012160	0.234119	0.093636	249.97	0.013360	0.137857	0.055150
	800.10	0.012300	0.291514	0.036435	800.15	0.019000	0.506560	0.063308
	499.70	0.059960	0.374498	0.074945	499.81	0.038320	0.372019	0.074432
1%	250.07	0.029920	0.174642	0.069836	250.07	0.029360	0.075548	0.030210
	1204.24	0.353617	0.687151	0.057061	1203.95	0.329233	3.437451	0.285514
	795.02	0.622575	0.595703	0.074929	798.05	0.244225	1.725383	0.216201
	249.25	0.300240	0.195939	0.078612	248.87	0.453280	0.184090	0.073971
	798.49	0.188825	0.509036	0.063750	800.19	0.023825	3.086776	0.385755
2%	501.88	0.375000	0.379417	0.075600	499.20	0.159080	1.587343	0.317975
	250.63	0.252560	0.141943	0.056634	250.42	0.169200	0.104346	0.041668
	1197.99	0.167267	0.732889	0.061176	1206.00	0.499717	0.123099	0.010207
	798.46	0.191975	0.841179	0.105350	791.48	1.064950	0.591440	0.074726
	249.22	0.310400	0.196106	0.078687	254.75	1.901280	0.246544	0.096777
	810.39	1.298475	0.379791	0.046865	802.53	0.316850	0.266825	0.033248
	495.44	0.911720	0.453134	0.091461	497.90	0.420080	0.435118	0.087391
	251.24	0.494400	0.155987	0.062088	248.58	0.567120	0.229260	0.092227

Table 2.

Results of the calculations for the sensors in position C (continuation; notations the same as in Table 1)

Per.	$\alpha$	$e$ [%]	$\sigma$	$\sigma^p$ [%]	$\alpha$	$e$ [%]	$\sigma$	$\sigma^p$ [%]
	4s				8s			
0%	1200.33	0.027233	0.523021	0.043573	1200.21	0.017567	0.633615	0.052792
	799.76	0.030550	0.400329	0.050056	799.89	0.014000	0.575772	0.071982
	250.02	0.009040	0.105485	0.042190	250.03	0.012560	0.170609	0.068235
	799.81	0.023575	0.365162	0.045656	799.83	0.021650	0.258956	0.032376
	500.14	0.028600	0.176385	0.035267	500.10	0.019920	0.389838	0.077952
	250.03	0.011120	0.083975	0.033586	250.00	0.000160	0.141152	0.056461
1%	1198.28	0.143750	1.417643	0.118307	1197.83	0.180533	0.491067	0.040996
	798.44	0.194675	1.115284	0.139682	802.44	0.305450	0.646330	0.080545
	251.56	0.622160	0.174450	0.069348	249.73	0.109440	0.121669	0.048721
	807.81	0.976050	0.917404	0.113567	806.36	0.795250	0.260953	0.032362
	499.46	0.108400	0.788288	0.157829	495.33	0.933680	0.431558	0.087125
	248.43	0.626480	0.121246	0.048804	250.26	0.105920	0.128759	0.051449
2%	1204.12	0.343533	1.196884	0.099399	1200.19	0.015900	3.626583	0.302167
	799.05	0.118525	0.901766	0.112855	787.92	1.510525	2.071161	0.262866
	248.58	0.569440	0.318893	0.128288	249.52	0.193280	0.085336	0.034200
	800.72	0.090375	0.355781	0.044433	804.02	0.502675	0.636905	0.079215
	497.93	0.413640	0.492764	0.098962	508.53	1.705120	0.284324	0.055911
	247.93	0.828960	0.274737	0.110814	249.56	0.177280	0.099899	0.040030

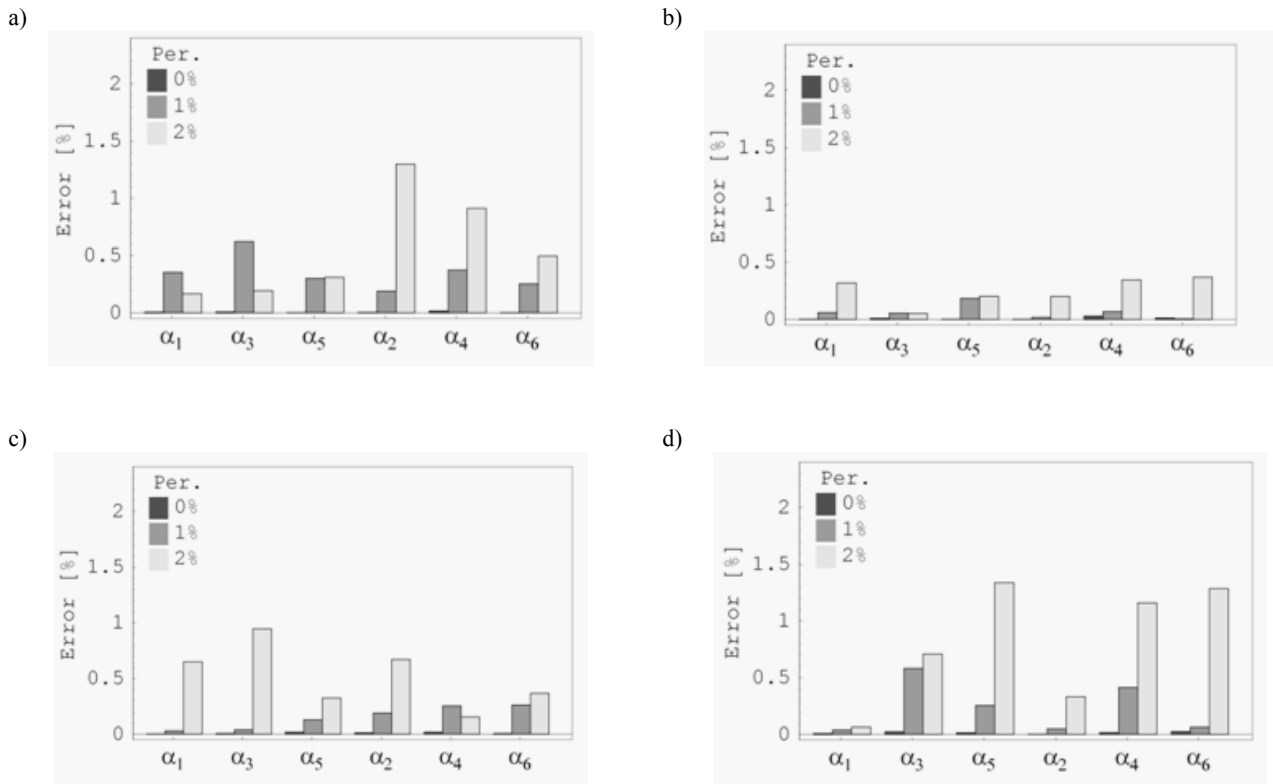


Fig. 4. Errors in the reconstruction of the heat transfer coefficient for the calculation for the sensors in position A and control performed every single second (a), every two seconds (b), four seconds (c) and eight seconds (d)

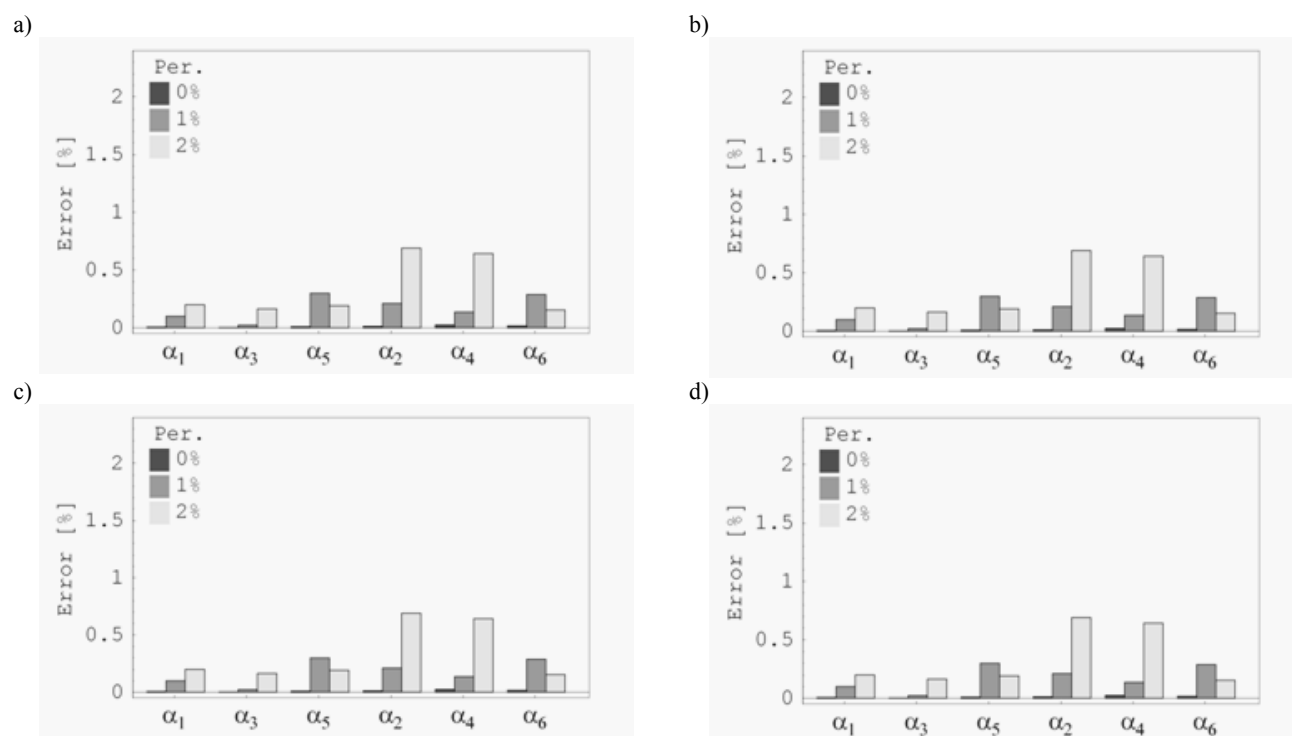


Fig. 5. Errors in the reconstruction of the heat transfer coefficient for the calculation for the sensors in position B and control performed every single second (a), every two seconds (b), four seconds (c) and eight seconds (d)

In Figure 6 the exact and reconstructed temperature distributions at the control points for the calculations of the sensors in position C, are shown, with the perturbation equal to 2%, and for the temperature control performed every two seconds (a and b) and every eight seconds (c and d). In the case of temperature control performed every eight seconds, the mean relative percentage error of temperature reconstruction (in comparison with the exact data) was 0.0542%. In such case, the maximal relative percentage error at a single control point was 0.1869%, maximal absolute error was 2.78 [K], whereas the mean maximal error equalled 0.65 [K]. For the sensors in position A the mean relative percentage error of temperature reconstruction was equal to 0.0809%, the maximal relative percentage error at a single control point was 0.1411%, the maximal absolute error was equal to 1.4 [K], whereas the mean absolute error was 0.84 [K]. For the sensors in position B these errors were: 0.0321%, 0.3292%, 4.82 [K] and 0.39 [K], respectively. Thus, in each of the examined cases, similar errors values were obtained. For a bigger number of control points and smaller perturbation, the exactness of temperature reconstruction at the control points was even better.

## 5. Conclusions

In the paper the method of the calculation of the cooling condition in the two-dimensional solidification processes is presented. Considered problem consists in the reconstruction of the function that describes the heat transfer coefficient on the boundary, when the temperature measurements in selected points of the solid phase are well-known. In calculations the alternating

phase truncation method, the genetic algorithm and the Tikhonov regularization were used.

The results indicate that for the exact input data, the function describing the cooling conditions is reconstructed with minimal error, which may be further reduced by changing the criterion of ending the genetic algorithm (increasing the maximal number of generations). The values of the errors are also affected by the number of control points (the points at which temperature values are known) and by the values of the errors in the input data. The reduction of the number of control points and increase of the size of the errors (generally) lead to worse reconstruction of the heat transfer coefficient; however, in each single case, the errors in the reconstruction of the cooling conditions are smaller than the input data errors. It may be concluded on the bases of the results that every start-up of the genetic algorithm leads to similar results, which are reflected by very low values of the standard deviation. The calculations, of which only a part was discussed in this paper, also point to the stability of the proposed method in view of the input data errors, number of control points, substantiating the usability of such approach.

## Acknowledgements

The research was financed by resources allocated in years 2007-2009 under the research project no. N N512 3348 33. The calculations were made at the Warsaw University Interdisciplinary Centre for Mathematical and Computational Modelling (ICM) under computational grant no. G30-7.



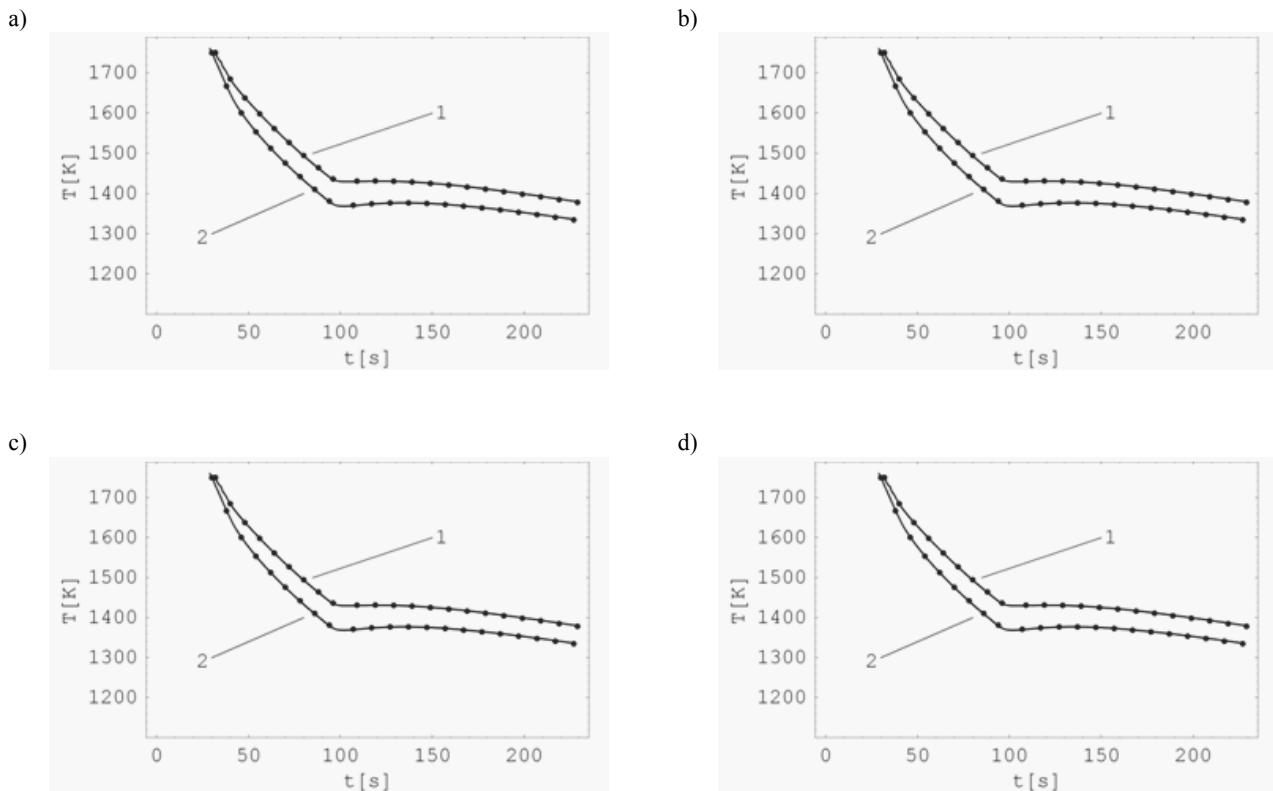


Fig. 6. Exact (solid line) and reconstructed (dots) distributions of the temperature at the measurement points for the calculations of the sensors in position C, perturbation equal to 2%, and for the temperature control performed every two seconds (a and b) and every eight seconds (c and d)

## References

- [1] D. Colton, The inverse Stefan problem for the heat equation in two space variables, *Mathematika* 21 (1974) 282-286.
- [2] R. Grzymkowski, D. Słota, Optimization method for one- and two-dimensional inverse Stefan problems, *Proceedings of the 3<sup>rd</sup> International Conference "Inverse Problems in Engineering"* ASME//UEF, New York, 1999, 1-11.
- [3] R. Grzymkowski, D. Słota, Approximation method for inverse Stefan problems, *Proceedings of the 16<sup>th</sup> IMACS World Congress, IMACS, Lausanne, 2000*, 1-4.
- [4] R. Grzymkowski, D. Słota, The inverse problems in the thermal theory of foundry - Identification of the parameters of solidification, *Proceedings of the 4<sup>th</sup> International ESAFORM Conference "Material Forming"*, Universite de Liege, Liege, 2001, 415-418.
- [5] R. Grzymkowski, D. Słota, One-phase inverse Stefan problems solved by Adomian decomposition method, *Computers and Mathematics with Applications* 51 (2006) 33-40.
- [6] P. Jochum, The numerical solution of the inverse Stefan problem, *Numerische Mathematik* 34 (1980) 411-429.
- [7] P. Jochum, To the numerical solution of an inverse Stefan problem in two space variable, *Numerical Treatment of Free Boundary Value Problems*, Birkhauser, Basel, 1982, 127-136.
- [8] S. Kang, N. Zabaras, Control of freezing interface motion in two-dimensional solidification processes using the adjoint method, *International Journal for Numerical Methods in Engineering* 38 (1995) 63-80.
- [9] K. Kurpisz, A.J. Nowak, *Inverse Thermal Problems*, Computational Mechanics Publications, Southampton, 1995.
- [10] J. Liu, B. Guerrier, A comparative study of domain embedding methods for regularized solutions of inverse Stefan problems, *International Journal for Numerical Methods in Engineering* 40 (1997) 3579-3600.
- [11] E. Majchrzak, B. Mochnacki, Application of the BEM in the thermal theory of foundry, *Engineering Analysis with Boundary Elements* 16 (1995) 99-121.
- [12] Z. Michalewicz, *Genetic Algorithms + Data Structures = Evolution Programs*, Springer-Verlag, Berlin, 1996.
- [13] A. Osyczka, *Evolutionary Algorithms for Single and Multicriteria Design Optimization*, Physica-Verlag, Heidelberg, 2002.

- [14] J.C.W. Rogers, A.E. Berger, M. Ciment, The alternating phase truncation method for numerical solution of a Stefan problem, *SIAM Journal on Numerical Analysis* 16 (1979) 563-587.
- [15] D. Słota, Three-phase inverse design Stefan problem, *Lecture Notes in Computer Science* 4487 (2007) 184-191.
- [16] D. Słota, Solving the inverse Stefan design problem using genetic algorithms, *Inverse Problems in Science and Engineering* 16/7 (2008) 829-846.
- [17] A.N. Tikhonov, V.Y. Arsenin, V.Y. Solution of Ill-Posed Problems, Wiley, New York, 1977.
- [18] N. Zabaras, Y. Ruan, O. Richmond, Design of two-dimensional Stefan processes with desired freezing front motions, *Numerical Heat Transfer B* 21 (1992) 307-325.
- [19] N. Zabaras K. Yuan, Dynamic programming approach to the inverse Stefan design problem, *Numerical Heat Transfer B* 26 (1994) 97-104.
- [20] D. Słota, Direct and inverse one-phase Stefan problem solved by variational iteration method, *Computers and Mathematics with Applications* 54 (2007) 1139-1146.